JOURNAL OF CATALYSIS 155, 43–51 (1995)

Skeletal Reactions of *n*-Hexane over Pt–NaY, Pt/SiO_2, HY, and Mixed Pt/SiO_2 + HY Catalysts

Zoltán Paál,* Zhaoqi Zhan,*,[2] István Manninger,* and W. M. H. Sachtler†,[1]

*Institute of Isotopes of the Hungarian Academy of Sciences, P.O. Box 77, H-1525 Budapest, Hungary; and †Center for Catalysis and Surface Science, Northwestern University, Evanston, Illinois 62007

Received September 16, 1994; revised February 6, 1995

The activity and selectivity of three samples of 8% Pt–NaY calcined at 633, 723, and 823 K, respectively, have been probed with *n*-hexane as the model reactant at 603 K and subatmospheric pressures in a glass closed-loop reactor. These catalysts were compared with 6.3% Pt/SiO_2 (EUROPT-1), HY, and a physical mixture of the latter two. The activity of all Pt–NaY catalysts is superior to EUROPT-1 and they deactivate more slowly. The selectivity pattern of all Pt–NaY samples is closer to that characteristic of monofunctional Pt catalysts, as opposed to the pronounced acidic character of pure HY and the mechanical mixtures. The sample calcined at 633 K, which has the highest dispersion and probably contains Pt particles anchored to the support as $[Pt_n - H_x]^{x+}$ entities, shows the highest aromatization selectivity. The sample precalcined at 823 K with the lowest dispersion has a pronouncedly high skeletal isomerization selectivity. The isomerization pathway may be related to the C_5 cyclic route on metal sites that are more abundant on the larger crystallites of this catalyst and are more easily accessible with its partially collapsed zeolite framework. Characteristic differences between samples in the response of their catalytic performance to changes in hydrogen and hydrocarbon pressure are discussed.

INTRODUCTION

Platinum catalysts supported on nonacidic zeolites represent a new, monofunctional aromatization catalyst for *n*-hexane (1, 2). The properties of these catalysts have been explained either by zeolite geometry or by various electronic interactions between platinum and zeolite. For example, the influence of zeolite pore geometry on the selectivity of methylcyclopentane (MCP) ring openings was observed over Pt–NaY catalyst (3). Deactivation of metal sites in the narrow zeolite pores was slower, since they present unfavorable geometry for polymerization of unsaturated coke precursors (4). The interaction of metal centers with the basic sites of the zeolite framework has been claimed to promote aromatization (5–7). This effect is not restricted to zeolitic supports (8, 9).

The *in situ* reduction of Pt ions in zeolites creates a situation different from other systems. Reduction with H_2 of an oxidized Pt precursor in Pt black or Pt/SiO_2 will produce water as the co-product:

$$PtO + H_2 \rightarrow Pt + H_2O.$$

On zeolites, however, protons are always created when metal ions are reduced with H_2 (10, 11):

$$Pt^{2+} + H_2 \rightarrow Pt^0 + 2\,H^+.$$

These protons are produced in the vicinity of metal sites and form chemical bonds with them (11, 12):

$$Pt_n + xH^+ \rightarrow [Pt_n - H_x]^{x+}.$$

The presence of such entities may explain the presence of "electron-deficient Pt particles" supposedly present on a zeolite support (13). The $Pt–H–O_{zeolite}$ bond anchors the Pt_n particle to the support. These combined $[Pt_n–H_x]^{x+}$ sites also exhibit peculiar catalytic propensities; for example, the bifunctional pairs of metal–acid active sites atomically close to each other offer a novel bifunctional route for aromatization by a C_5 ring enlargement route without shuttling the intermediates between metal and acid sites (11). These sites also have an intrinsically lower activity in MCP ring openings (12). Ring enlargement due to $[Pt_n–H_x]^{x+}$ clusters was minor or absent with Pd supported on NaY, as opposed to Pd/HY (11).

Three types of Pt–NaY catalysts with platinum particles located in different positions of the zeolite have been obtained by employing different calcination temperatures prior to reduction at 723 K (14–16). Small Pt particles in the supercages were produced by a calcination at 633 K,

[1] To whom correspondence should be addressed.

[2] On leave from Lanzhou Institute of Physical Chemistry, Academia Sinica, Lanzhou, PR China. Present address: Faculty of Chemical Technology, University of Twente, P.O. Box 217, 7500 AE Enschede, The Netherlands.

0021-9517/95 $12.00

"grape-like" particles extending over a number of cavities were obtained at 723 K, while the calcination at 823 K resulted in rather large Pt crystallites supposedly at the outer surface of the support grains (14, 16). Alternatively, the zeolite structure may collapse as a result of Pt particles outgrowing the space within the framework (17), the metal particles becoming thus more accessible to the reactants. Hence Pt–mordenite catalysts of lower metal dispersion showed higher activity in *n*-heptane reactions (17).

In the present study, *n*-hexane was used as the model hydrocarbon. Pt sites catalyze its isomerization, C_5 cyclization, aromatization, and fragmentation; these reactions are accompanied by dehydrogenation (18–21). Pt catalysts with an acidic zeolite support showed a high isomerization selectivity, whereas C_5 cyclization and aromatization prevailed on Pt supported on basic zeolites (6). Pt–KL catalyst reduced by H_2 produced more isomers than Pt–KL reduced by $NaBH_4$ or a Pt–KL catalyst treated subsequently with KNO_3 (20). The geometric constraint exerted on the reactant molecules (hence, the expected deactivation (4)) and the metal–acid (or metal–base) structure at the molecular level should be different in these catalysts.

In this work, the interplay of the support and metal centers as well as catalyst geometry will be related to the catalytic properties of three Pt–NaY catalysts. These are compared with Pt/SiO_2 (EUROPT-1), HY, and their mechanical mixture in order to distinguish between the effect of anchored bifunctional clusters and that of acid and metal centers separated in space (11).

EXPERIMENTAL

Catalysts and Their Pretreatment

Pt–NaY was prepared by an ion exchange method at Northwestern University; details of its preparation and characterization were reported earlier (16). Before catalytic runs, each sample was calcined in O_2 with a flow rate of 1000 ml min^{-1} g^{-1}, raising the temperature from 300 K to its final value (T_c = 633, 723, and 823 K, respectively) at a heating rate of 30 K h^{-1}. Samples were kept for 2 h at T_c before being cooled. The subsequent reduction was carried out in a mixture of 5% hydrogen, 95% nitrogen at a flow rate of 30 ml min^{-1} g^{-1} from 300 to 773 K at 10 K min^{-1}. The final calcination temperature determines the location and dispersion of platinum in Y-zeolite (14–16). The three types of Pt–NaY catalysts are denoted PtY-633, PtY-723, and PtY-823. Their platinum content is 8.6%, as determined by atomic absorption spectroscopy (16). The metal dispersion, expressed by the atomic ratios of adsorbed hydrogen to platinum, H/Pt, have been reported to be 1.10, 0.60, and 0.30 for PtY-633, PtY-723, and PtY-823, respectively (16).

A standard 6.3% Pt/SiO_2 (EUROPT-1) (23) was used as a monofunctional metal catalyst. Its average platinum particle size is 1.8 nm, dispersion 60%. The sample was reduced in hydrogen flow at 673 K before use (21). The HY zeolite was a commercial sample from Russia. It has been pretreated in hydrogen at slow heating under oxygen to 573 K followed by a hydrogen treatment at 623 K (5).

Reactants

The purity of *n*-hexane (*n*H) was higher than 99.95%. The hydrogen was purified by passing it through a Pd–Ag thimble.

Catalytic Tests

The runs were performed in a glass closed-loop reactor (19, 22), with mixtures of *n*-hexane and hydrogen at 603 K. Small amounts, 1.3 to 5.2 mg, of Pt–NaY and EUROPT-1 were used. The mixed catalyst consisted of 2.3 mg of Pt/SiO_2 and 21 mg of HY. Samples were taken at various moments of the run (1 to 100 min after the start). No long duration tests have been carried out with the mixed catalyst. The catalysts were regenerated after each run with O_2 and H_2, as described earlier (21, 22). Sometimes, after longer runs, repeated regeneration cycles had to be applied to restore the initial activity and selectivity.

A Packard 437 type gas chromatograph with a capillary column (50 m by 0.32 mm fused silica, CP Sil 5 coating) was used for product analysis (18–20).

RESULTS

Activity

Figure 1a shows the absolute activity of the metal-containing catalysts, Pt–NaY, Pt/SiO_2, and Pt/SiO_2 + HY, at a pressure ratio $p(n\text{H}):p(H_2) = 10:120$. The titration results of Ref. (16) were used to calculate the amount of surface Pt atoms. The dispersion of PtY-633 was taken to be 1.0, disregarding the titration value of 1.1. All zeolite-supported catalysts were more active than EUROPT-1, the activity sequence being PtY-823 > PtY-633 > PtY-723. The mechanical mixture of HY and EUROPT-1 showed the highest level of activity.

Increasing the hydrogen pressure from 120 to 480 Torr (Fig. 1b) brought the activity of all Pt–NaY samples (and that of the mixed catalyst) close to each other. The activity of PtY-823 did not change much and that of the two other samples increased. The activity of EUROPT-1 was still far below that of the other samples.

Increasing both hydrogen and *x*-hexane pressure (keeping the *n*-hexane-to-hydrogen ratio constant at 1 : 12) accelerated the conversion of *n*-hexane over all zeolitic samples. PtY-823 and PtY-723 were the most active, although the latter started to deactivate earlier (Fig. 1c). The perfor-

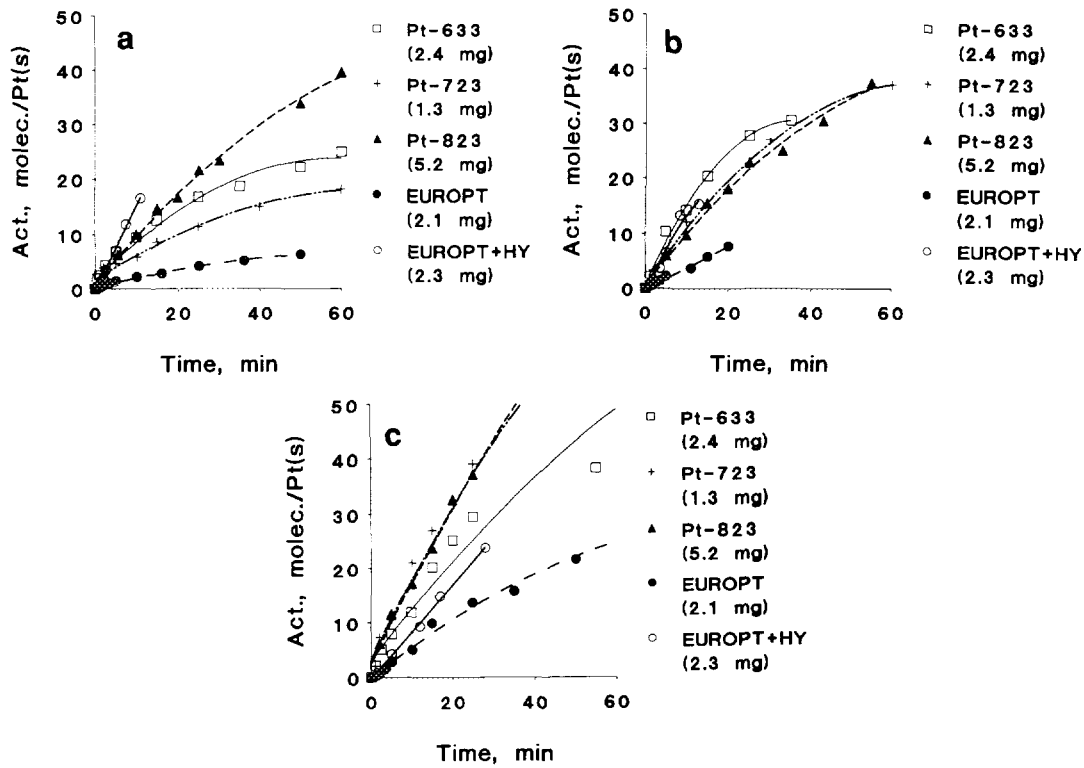

FIG. 1. Specific activity of the five catalyst samples (expressed as transformed hexane molecules per surface Pt atom) as a function of the reaction time. (a) $p(n\mathrm{H}):p(\mathrm{H_2}) = 10:120$, (b) $p(n\mathrm{H}):p(\mathrm{H_2}) = 10:480$, (c) $p(n\mathrm{H}):p(\mathrm{H_2}) = 40:480$. Note that the same scale is used in all three cases but there are results up to $t = 100$ min for Fig. 1c, and the fitting used also points outside the range depicted.

mance of the mixed catalyst was behind the zeolite-supported samples. EUROPT-1 had again the poorest activity at about the same level as observed at 10 : 480. The activity of PtY-823 was almost the same at the lowest hydrogen excess (40 : 120), as in Figure 1c, while that of all other catalysts was considerably lower. The activity of the mixed catalyst showed a less marked hydrogen and hydrocarbon pressure dependence.

The deactivation rates shown in Table 1 for two pressure ratios have been estimated by fitting a second-order polynomial to the curves in Fig. 1 in their initial section. The most rapid deactivation with PtY-633 is confirmed, while both PtY-723 and PtY-823 deactivated more slowly. The lower deactivation rates at $p(n\mathrm{H}):p(\mathrm{H_2}) = 40:480$ are clearly seen.

Selectivity

a. Initial selectivities. Plotting selectivities as a function of the conversion (S–X curves) permits one to distinguish between primary and secondary products (24). Figure 2 compares the Pt–NaY catalysts at $p(n\mathrm{H}):p(\mathrm{H_2}) = 10:120$. Although overall rates were nearly identical with PtY-723 and PtY-823 (cf. Fig. 1a), rather different selectivity patterns appeared. Hexenes with the highest selectivity at the lowest conversions are primary products. PtY-633 seems to possess an inherent aromatization ability in the first moments of the run, while initial C_5 cyclization and fragmentation behavior appeared with PtY-723 and PtY-823. With dropping olefin selectivity, methylcyclopentane becomes one of the predominant products on PtY-633 and PtY-723 (together with benzene). Skeletal isomers predominate on PtY-823 even initially.

The mixed catalyst (Fig. 3) exhibited some low, intrinsic

TABLE 1

Deactivation Rates of Various Catalysts

Catalyst	Pressure ratio $n\mathrm{H}:\mathrm{H_2}$ (Torr)	Deact. rate[a] ((Δ%) $\mathrm{min^{-1}}$)
Pt-633	10 : 120	−4.2
	40 : 480	−0.93
Pt-723	10 : 120	−0.53
	40 : 480	−0.39
Pt-823	10 : 120	−0.53
	40 : 480	−0.47

[a] Percent change of the reaction rate per minute up to an overall conversion of 10%, by fitting a second order polynomial. The amount of molecules transformed per surface Pt atom at this conversion is ca. 14 at $p(n\mathrm{H}) = 10$ Torr and ca. 55 at $p(n\mathrm{H}) = 40$ Torr.

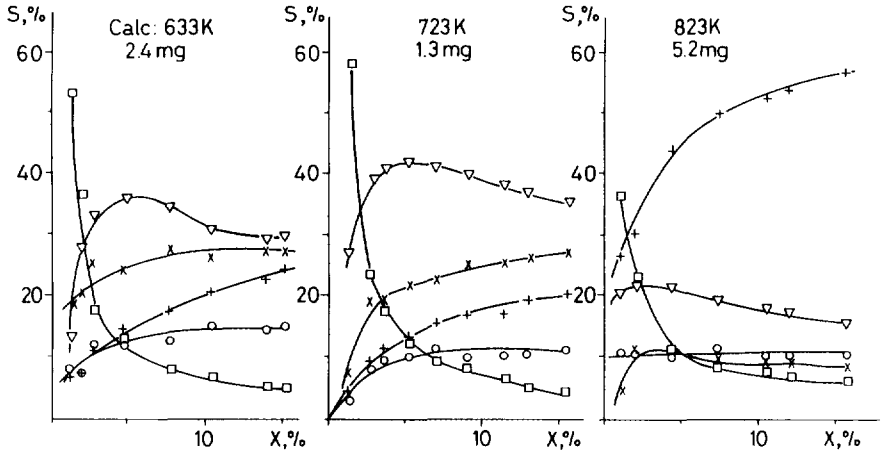

FIG. 2. Selectivity for various product classes over three Pt–NaY (8%) samples and Pt black (presintered at 473 K) as a function of the overall conversion at pressure ratio $p(n\mathrm{H}):p(\mathrm{H_2}) = 10:120$. Symbols: ○, $<C_6$; +, isomers; ▽, methylcyclopentane; □, hexenes; ×, benzene.

initial C_5 cyclization and aromatization activity but fragmentation became more and more important at higher conversions.

Skeletal isomers were major products at all pressure ratios over PtY-823, as shown in Fig. 4, where a similar graph for Pt black has been included for $p(n\mathrm{H}):p(\mathrm{H_2}) = 40:480$. A high initial and rapidly decreasing hexene selectivity was characteristic at other $p(n\mathrm{H}):p(\mathrm{H_2})$ ratios as well, especially at $p(n\mathrm{H}):p(\mathrm{H_2}) = 40:120$. At $p(n\mathrm{H}):p(\mathrm{H_2}) = 10:480$, in turn, all products seemed to be primary.

b. Selectivities in the stabilized state. The three Pt–NaY catalysts showed a more similar selectivity pattern in their stabilized state (Table 2). The amount of hexenes was minor and the fragmentation selectivities were similar. Of all Pt–NaY catalysts, PtY-633 produced the most benzene. Its selectivity decreased gradually with higher calcination temperatures. The abundance of isomers showed the reverse sequence; the highest isomerization selectivity of PtY-823 is clearly seen. Skeletal isomers consist mainly of methylpentanes (MP), together with 2,3-dimethylbutane (2,3DMB) with selectivities in the range of 1 to 2%. EUROPT-1 produced roughly 0.5% 2,3DMB while its selectivity could reach 5% with Pt on acidic

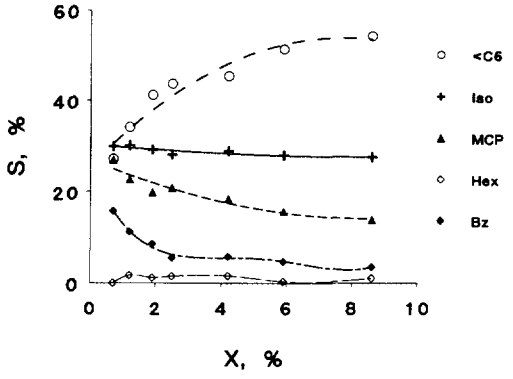

FIG. 3. Selectivity for various product classes over mixed EUROPT-1 + HY catalyst as a function of the overall conversion. Pressure ratio $p(n\mathrm{H})/p(\mathrm{H_2}) = 10:120$.

TABLE 2

Summarized Results on the Selectivity of *n*-Hexane Reactions

Catalyst	Conv. (%)	Selectivity (%)				
		$<C_6$	Iso	MCP	Bz	Hex
A. $n\mathrm{H}:\mathrm{H_2} = 10:480$						
PtY-633	23	18	37	17	26	2
PtY-723	22	19	41	17	20	3
PtY-823	22	17	52	18	12	1
EUROPT-1	10	8	52	28	11	1
EUROPT-1+HY	6	30	46	18	6	tr.
HY	0.7	84	16	—	—	—
	3.5	82	17	1	—	tr.
B. $n\mathrm{H}:\mathrm{H_2} = 10:120$						
PtY-633	15	15	23	30	27	5
PtY-723	15	16	36	26	18	4
PtY-823	16	12	57	16	9	6
EUROPT-1	8	8	21	46	17	8
EUROPT-1+HY	6	51	28	16	5	tr.
HY	0.6	81	19	—	—	—
	3.6	82	17	1	—	tr.
C. $n\mathrm{H}:\mathrm{H_2} = 40:120$						
PtY-633	12	10	39	22	19	10
PtY-723	7	9	23	32	21	15
PtY-823	20	8	72	6	4	10
EUROPT-1	4.5	7	10	35	13	35
EUROPT-1+HY	11	56	38	4	1	1
HY	0.5	59	39	2	—	—
	7	65	34	0.5	—	0.5

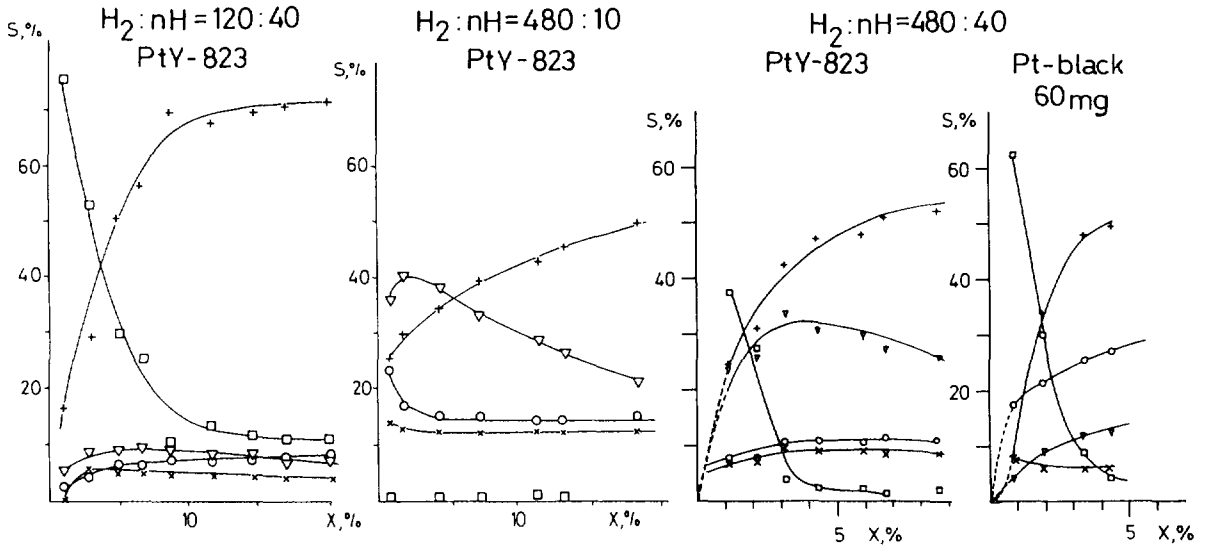

FIG. 4. Selectivity for various product classes over PtY-823 at three different $p(n\mathrm{H}):p(\mathrm{H_2})$ ratios, together with selectivity over Pt black (presintered at 473 K) at $p(n\mathrm{H}):p(\mathrm{H_2}) = 40:480$, as a function of the overall conversion. Symbols as in Fig. 2.

support (6). Figure 5 shows that the ratio of 2,3DMB/MP *decreases* with higher precalcination temperature (17).

Hydrogen and hydrocarbon pressure effects have also been included in Table 2. Higher $p(\mathrm{H_2})$ favored hydrogenolysis and hampered dehydrogenation. No straightforward correlation was observed with the other products. Benzene selectivity was not suppressed by higher hydrogen pressures. The high isomerization and low methylcyclopentane selectivity over PtY-823, especially at $p(n\mathrm{H}):p(\mathrm{H_2}) = 40:120$, is worth mentioning.

The mixture of EUROPT-1 and HY gave rise to pronounced amounts of C_6 products with rather high amounts of fragments. More hydrogen in this case favored nondestructive reactions.

The HY catalyst exhibited high selectivity for fragmentation, but isomers and traces of other products were also formed. The degradative selectivity was lowest at $p(n\mathrm{H})):p(\mathrm{H_2}) = 40:120$. Selectivities at two conversion values shown for HY indicate that the values are fairly constant and, in most cases, independent of the conversion.

The distribution of fragments shown in Table 3 indicates a predominant random or "internal" fission over Pt–NaY catalysts and EUROPT-1. This is characteristic of metal-catalyzed hydrogenolysis and is confirmed also by the M_f value (25) being higher than unity. A preference for propane formation, reported also with other Pt catalysts (18, 19, 21), is evident, ethane and butane being formed in nearly equal but smaller amounts. Clarke *et al.* attributed terminal scission to electron-rich Pt sites (26). They reported preferential internal scission of *n*-pentane for chlorine-free Pt/MgO catalysts (27). Approximately the same amounts of complementary fragments were produced in both cases mentioned, as opposed to the present study where the methane excess indicated that a multiple splitting may have been superimposed on the predominant

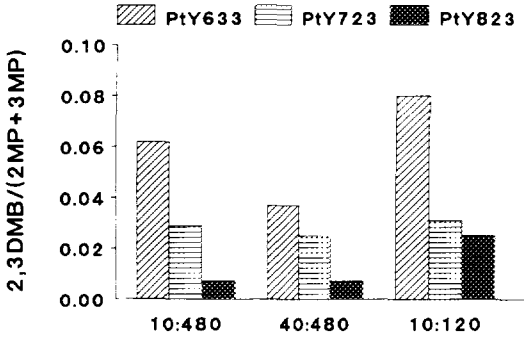

FIG. 5. Ratio of 2,3-dimethylbutane to the sum of methylpentanes (2,3DMB/MP) over various Pt–NaY catalysts, at different $p(n\mathrm{H}):p(\mathrm{H_2})$. Conversion: 10 ± 1%.

TABLE 3

Distribution of Fragments from *n*-Hexane, $n\mathrm{H}:\mathrm{H_2} = 10:120$

Catalyst	Conv. (%)	Fragment distribution					
		C_1	C_2	C_3	C_4	C_5	M_f[a]
PtY-633	7	37	15	18	13	17	4.1
PtY-723	9	33	16	20	15	16	5.2
PtY-823	7	32	17	21	15	15	5.6
EUROPT-1	7	33	16	24	14	13	5.4
EUROPT-1+HY	5	5	4	58	19	14	45
HY	4	3	3	58	22	15	83

[a] $M_f = \Sigma(C_2–C_5)/CH_4$ (25).

TABLE 4

Characteristic Product Ratios [$p(n\text{H}):p(\text{H}_2) = 10:120$]

Catalyst	Conv. (%)	Ratio			
		MCP/Iso	Bz/C_6 sat.	$<C_6/C_6$	2MP/3MP
PtY-633	7.6	2.0	0.53	0.15	1.32
PtY-723	6.9	2.7	0.40	0.13	1.64
PtY-823	7.3	0.74	0.19	0.14	1.43
EUROPT-1	8.2	2.2	0.29	0.092	1.94
EUROPT-1+HY	8.6	0.50	0.082	1.18	1.61
HY	4	0.06	0	4.8	1.71
0.8% Pt–NaY[a]	7.7	3.1	0.75	0.115	1.92
0.8% Pt–NaX[a]	8.0	3.0	0.29	0.104	1.82
0.8% Pt–KL[b]	7	3	0.4	0.15	1.3
0.8% Pt–KL+K[b,c]	7	5	0.5	0.13	1.4

[a] Taken from Ref. (6).
[b] Taken from Ref. (20), catalyst reduced by H_2. Data extracted from figures.
[c] Catalyst treated with KNO_3 solution.

single rupture. This situation was similar to that found with EUROPT-1 (18). The possible difference in the electric charge of Pt particles in our three samples did not seem to influence the fragment composition. Hardly any methane was formed and the value of M_f was very high whenever HY was present, pointing to a prevailing acid-catalyzed cracking (28, 29).

Table 4 compares a few product ratios calculated at the beginning of the stabilized stage of all present catalysts with similar values observed over other Pt–zeolite catalysts. PtY-633 and PtY-723 were closest to EUROPT-1; the formation of MCP was even higher over PtY-723 than on Pt/SiO_2. PtY-823 produced not only more isomers but also less MCP than the others. The ratios 2MP/3MP were below the statistical value of 2. It showed no clear-cut dependence on pretreatment temperature or on the hydrogen or hydrocarbon pressure, as opposed to that reported for EUROPT-1 (18). The ratios obtained over Pt–NaY also over other Pt/zeolites were different from those observed in the presence of HY.

DISCUSSION

Significant activity differences are seen between various Pt–NaY samples. Remarkably, the activity per unit mass of Pt was higher with samples of lower metal dispersion; a similar result was reported and interpreted in Ref. (17). The overall activity of Pt/zeolite catalysts was not far from that of the physical mixture of EUROPT-1+HY, although the state of metal particles and the relative position of metal and acidic sites were certainly different. Thus, bifunctionality may increase the activity but mere activity results cannot give a final answer on the likely nature of the active sites (metals, acids, or combined $[Pt_n–H_x]^{x+}$ clusters).

The responses in overall activity of various catalysts to hydrogen and hydrocarbon pressure changes were not the same. With EUROPT-1, the ratio of *n*-hexane and H_2 pressure was less important (19, 21) than the absolute hydrogen pressure. We found a reverse situation here. The rates were much higher and more stable at $p(n\text{H}):p(\text{H}_2) = 40:480$ (and 10 : 480) than at 10 : 120. This effect of higher hydrogen pressure has been attributed to the competition between H_2 and hydrocarbons for surface sites (30). The superiority of Pt–NaY catalysts over the mechanical mixture appears mainly at higher *n*-hexane and hydrogen pressures (Figs. 1b and 1c).

The relative activity and deactivation rates of the three Pt–NaY samples are in good agreement with the suggestion (17) that a better accessibility of metal sites in a partially collapsed zeolite framework results in higher levels of activity. As reported by Jaeger *et al.* (31), growing metal particles can induce a local collapse of the zeolite framework in Pt-loaded Na*X* catalysts. This phenomenon was not considered in some older work (16). This collapse starts even after a pretreatment at 723 K and should be pronounced in PtY-823 where the Pt crystallites should be situated in a partly destroyed zeolite pore system rather than on the outer surface of the support grains. The highest activity of these samples is most obvious at $p(n\text{H}):p(\text{H}_2) = 40:480$ (Fig. 1c). A fourfold increase in *n*-hexane pressure did not affect the activity of PtY-633, where its diffusion to the small Pt particles through zeolite pores can be most important, but its slower deactivation rate, as predicted in Ref. (4), manifested itself (Figs. 1b vs 1c, and Table 1). For the sake of clarity we ought to

mention that pore diffusion control can affect the local reactant/product ratio in the steady state whereas the ratio H_2/hydrocarbon will remain almost independent of the location.

The selectivity pattern of HY (Table 2) illustrates that its pure (and strong) acidic sites produce mainly fragments and some skeletal isomers under our conditions. Pure metal sites of EUROPT-1 give mainly C_6-saturated products (18, 19, 21) with lower fragmentation and aromatization selectivities (ca. 10% each).

The general selectivity pattern of Pt–NaY catalysts shows several analogies with EUROPT-1 (Tables 2 and 3). All products that could have formed over metal sites appear also on Pt–zeolites. The hydrogen pressure dependence and the initial changes of selectivities were similar and so was the fragment distribution.

The high aromatic selectivity of PtY-633 is in agreement with the predicted ability of small Pt particles to promote C_6 dehydrocyclization (4, 9, 23, 32). These small particles can be anchored to the support via $[Pt_n–H_x]^{x+}$ entities. An increase of benzene formation parallel to the decrease of MCP selectivity with both PtY-633 and PtY-723 may point to the novel bifunctional aromatization route via $C_5 \rightarrow C_6$ ring enlargement (11) as an additional aromatization pathway (Fig. 2). The abundance of $[Pt_n–H_x]^{x+}$ clusters must be lower here than in metals supported on HY (11, 12). The present catalysts may be analogous to Pd–NaY, which exhibits mainly metallic properties (with a 90% ring opening and 10% ring enlargement selectivities) at the beginning of the run (11). The anchoring function of the protons, in turn, can still exist, obviously with the excess metallic Pt in the clusters, i.e., n being much higher than x in $[Pt_n–H_x]^{x+}$ entities.

Aromatization over PtY-633 is somewhat superior to the Pt–KL sample treated with K^+ ions (Table 4), which exhibited the highest benzene selectivity of several Pt–KL samples (20). The best aromatizing catalyst of all samples listed in Table 4 was a 0.8% Pt–NaY (6). Its lower metal loading gave rise, probably, to still smaller Pt particles, and hence it produced more benzene (Table 4). At the same time, the relative amount of benzene over all 8% Pt–NaY catalysts was higher than on a highly basic 0.8% Pt–NaX (6). Hence, we believe that the basic support is not the only factor promoting aromatization; the slower deactivation of the small Pt crystallites may be more important, as was proposed by Iglesia and Baumgartner (4).

Benzene formation via a stepwise dehydrogenation of hexane followed by ring closure has been proposed for monofunctional metals (33). In addition, a "direct" route of aromatization seemed to appear at higher hydrogen excess (34). Likewise, direct aromatization seems to occur in the first period of reaction over all Pt–NaY catalysts. The ability of the mixed (HY plus EUROPT-1) catalyst to produce benzene and MCP in addition to isomers and fragments is clearly seen in Fig. 3. This reaction is probably making use of the traditional bifunctional route.

The main pathway of isomerization over metal centers involves surface cyclopentane-like intermediates (35). They may desorb as methylcyclopentane or as methylpentanes. Since this latter reaction requires the uptake of two hydrogen atoms, a higher hydrogen excess favors isomerization (30), cf. Table 2. The actual hydrogen availability on the metal sites is lower with smaller particles, hence smaller MCP/isomer ratios appeared on PtY-823 than on PtY-723. EUROPT-1 and other Pt–zeolite samples (6, 20) produced more MCP (Table 4). The selectivity pattern of PtY-723 was closest to that observed with EUROPT-1 (18, 19, 21), with MCP being still more abundant on PtY-723 (Table 4).

In addition, another route may contribute to isomerization on Pt–NaY catalysts of higher dispersion, probably with the participation of $[Pt_n–H_x]^{x+}$ entities, i.e., by an acid-catalyzed reaction. The amount of 2,3DMB is a good indicator of this pathway. Up to 5% 2,3-dimethylbutane selectivity had been observed with Pt on an acidic support (6), with the 2,3DMB/MP ratio being about 0.15. The value of an analogous ratio, viz. multiple-branched/monobranched isomers from *n*-heptane over Pt–mordenite catalysts, was between 0.13 and 0.19. It decreased as the dispersion of Pt decreased and the metallic character of the catalyst became more pronounced (17). In the present study, the 2,3DMB/MP ratio was significantly lower (Fig. 5). The abundance of 2,3DMB decreased in the sequence PtY-633 > PtY-723 > PtY-823, as did the possible contribution of acidic centers in isomerization. This decrease in acidity is likely to be accompanied by the local collapse of the zeolite framework as reported in Ref. (17) and an enhancement of the metallic character of the catalyst.

PtY-823 exhibited an outstandingly high isomerization and low MCP selectivity (Tables 2 and 4). A direct *n*-hexene → methylpentane reaction can occur with the lowest hydrogen excess, i.e., $p(n\text{H}):p(\text{H}_2) = 40:120$ in the initial period of the run (Fig. 4). The selectivity patterns point to a similar reaction on Pt black with more hydrogen present (i.e., at $p(n\text{H}):p(\text{H}_2) = 40:480$ (Fig. 4)) since higher $p(\text{H}_2)$ is necessary to maintain a similar surface hydrogen abundance on that catalyst. (One has to recall the enhanced alkene formation also from *n*-pentane over Pt/TiO_2 with low hydrogen excess (26).) A MCP → isomer route gradually displaces the hexene → isomer reaction as hydrogen pressure increases. Isomerization over this catalyst is thus attributed to the metallic function. The relatively large Pt particles in this sample may contain sufficient surface hydrogen to accelerate the ring-opening step of isomerization while the zeolite framework prevents their deactivation (4).

The 2MP/3MP ratio (Table 4) being lower than the sta-

tistical value for all catalysts indicates some steric hindrance (3) in forming and decomposing the C_5 cyclic surface intermediate on all Pt–NaY catalysts. Clarke *et al.* (27) claimed that this ratio was determined by the initial point of attachment of the C_5 cyclic surface intermediate to the active sites. Similar ideas with somewhat different surface structures were put forward by one of the present authors (18, 36). The 2MP/3MP ratios over all three Pt–NaY catalysts were below 2, i.e., lower than the values near 2 with EUROPT-1 (Table 4 and Ref. (18)) and much lower than those reported with Pt/MgO (up to ~3, Ref. (27)). This, in turn, may indicate that acidic centers also play some role in ring opening (37). Hence, our test reaction may, indeed, indicate a different primary attachment of the surface intermediate with Pt–NaY than with Pt/MgO. This is in good agreement with the expected reverse direction of charge transfer in the postulated $[Pt_n–H_x]^{x+}$ entities as opposed to that assumed with Pt/MgO (27).

CONCLUSIONS

Pt–NaY catalysts with 8% metal loading show mainly metallic character. All Pt–NaY catalysts exhibited higher overall activity than a monofunctional Pt/SiO_2(EUROPT-1). The higher activity of PtY-723 and especially PtY-823 as opposed to PtY-633 may be connected with the better accessibility of metal sites bought about by opening broader channels through the local collapse of the zeolitic framework (17). PtY-633, with the highest dispersion, shows the highest aromatization selectivity. $[Pt_n–H_x]^{x+}$ entities not only anchor the smallest Pt particles in PtY-633 but can also contribute to aromatization and skeletal isomerization on that sample and, to a minor extent, even on PtY-723. The latter showed a selectivity pattern closest to that of EUROPT-1. The pronounced isomer selectivity of PtY-823, the temporal evolution of which resembled that observed with unsupported Pt black, is attributed to its enhanced metallic properties.

ACKNOWLEDGMENT

W.M.H.S. gratefully acknowledges financial support from the National Science Foundation, Contract CTS-922/841.

REFERENCES

1. Bernard, J. R., *in* "Proceedings, 5th International Congress on Zeolites, Naples, 1980" (L. V. Rees, Ed.), p. 686. Heyden, London, 1980.
2. Hughes, T. R., Buss, W. C., Tamm, P. W., and Jacobson, R. L., *in* "New Developments in Zeolite Science and Technology" (Y. Murakami, a. Iijima and J. W. Ward, Eds.) p. 725. Kodansha, Tokyo/Elsevier, Amsterdam, 1986.
3. Moretti, G., and Sachtler, W. M. H., *J. Catal.* **116,** 350 (1989).
4. Iglesia, E., and Baumgartner, J. E., *in* "Proceedings, 10th International Congress on Catalysis, Budapest, 1992" (L. Guczi, F. Solymosi, and P. Tétényi, Eds.), Part B, p. 993. Elsevier, Amsterdam/Akadémiai Kiadó, Budapest, 1993.
5. De Mallmann, A., and Barthomeuf, D., *in* "Zeolites as Catalysts, Sorbents and Detergent Builders" (H. G. Karge and J. Weitkamp, Eds.), p. 429. Elsevier, Amsterdam, 1989.
6. Paál, Z., Zhan, Zh., Manninger, I., and Barthomeuf, D., J. Catal. **147,** 33 (1994).
7. Hicks, F., Han, W.-J., and Kooh, A. B., *in* "Proceedings, 10th International Congress on Catalysis, Budapest, 1992" (L. Guczi, F. Solymosi, and P. Tétényi, Eds.), Part B, p. 1043. Elsevier, Amsterdam/Akadémiai Kiadó, Budapest, 1993.
8. (a) Derouane, E. G., Jullien-Lardot, V., Davis, R. J., Blom, N., and Højlund-Nielsen, P. E., *in* "Proceedings, 10th International Congress on Catalysis, Budapest, 1992" (L. Guczi, F. Solymosi, and P. Tétényi, Eds.), Part B, p. 1031. Elsevier, Amsterdam/Akadémiai Kiadó, Budapest, 1993. (b) Baird, T., Kelly, E. J., Patterson, W. R., and Rooney, J. J., *J. Chem. Soc. Chem. Commun.* 1431 (1992). (c) Clarke, J. K. A., and Rooney, J. J., *in* "Proceedings, 10th International Congress on Catalysis, Budapest, 1992" (L. Guczi, F. Solymosi and P. Tétényi, Eds.), Part B, pp. 1040 and 1041. Elsevier, Amsterdam/Akadémiai Kiadó, Budapest, 1993.
9. Lafyatis, D. S., Froment, G. F., Pasau-Claerbout, A., and Derouane, E. G., *J. Catal.* **147,** 552 (1994).
10. Chow, M., Park, S. H., and Sachtler, W. M. H., *Appl. Catal.* **19,** 349 (1985).
11. Bai, X., and Sachtler, W. M. H., *J. Catal.* **129,** 121 (1991).
12. Bai, X., and Sachtler, W. M. H., *J. Catal.* **132,** 266 (1991).
13. Gallezot, P., *Catal. Rev. Sci. Eng.* **20,** 121 (1979).
14. Sachtler, W. M. H., Tzou, M. S., and Jiang, H. J., *Solid State Ionics* **26,** 71 (1988).
15. Park, S. H., Tzou, M. S., and Sachtler, W. M. H., *Appl. Catal.* **24,** 85 (1986).
16. Tzou, M. S., Teo, B. K., and Sachtler, W. M. H., *J. Catal.* **113,** 220 (1988).
17. Carvill, B. T., Lerner, B. A., Adelman, B. J., Tomczak, D. C., and W. M. H. Sachtler, *J. Catal.* **144,** 1 (1993).
18. Paál, Z., Groeneweg, H., and Paál-Lukács, J., *J. Chem. Soc. Faraday Trans. 1* **86,** 3159 (1990).
19. Paál, Z., Groeneweg, H., and Zimmer, H., *Catal. Today* **5,** 199 (1989).
20. Manninger, I., Zhan, Zh., Xu, X. L., and Paál, Z., *J. Mol. Catal.* **66,** 223 (1991).
21. Manninger, I., Zhan, Zh., and Muhler, M., *Appl. Catal.* **66,** 305 (1990).
22. Paál, Z., Räth, M., Zhan, Zh., and Gombler, W., *J. Catal.* **146,** 342 (1994).
23. Bond, G. C., and Paál, Z., *Appl. Catal.* **86,** 1 (1992).
24. Margitfalvi, J., Szedlacsek, P., Hegedüs, M., and Nagy, F., *Appl. Catal.* **15,** 69 (1985).
25. Ponec, V., and Sachtler, W. M. H., *in* "Proceedings, 5th International Congress on Catalysis, Palm Beach, 1972" (J. W. Hightower, Ed.) Vol. 1, p. 645. North-Holland, Amsterdam, 1973.
26. Clarke, J. K. A., Dempsey, R. J., Baird, T., and Rooney, J. J., *J. Catal.* **126,** 370 (1990).
27. Clarke, J. K. A., Bradley, M. J., Garvie, L. A., Craven, A. J., and Baird, T., *J. Catal.* **143,** 122 (1993).
28. Anderson, J. R., Foger, K., Mole, T., Rajadhyaksha, R. A., and Sanders, J. V., *J. Catal.* **58,** 114 (1979).
29. Haag, W. O., and Dessau, R. M., *in* "Proceedings, 8th International Congress on Catalysis, Berlin, 1984," Vol. 2, p. 305. Verlag Chemie, Weinheim, 1984.

30. (a) Paál, Z., *in* "Hydrogen Effects in Catalysis" (Z. Paál and P. G. Menon, Eds.), p. 449. Dekker, New York, 1988. (b) Paál, Z., *Catal. Today* **12,** 297 (1992).
31. Jaeger, N. I., Rathousky, J., Schulz-Ekloff, G., Svensson, A., and Zukal, A., *in* "Zeolites, Facts, Figures, Future" (P. A. Jacobs and R. A. van Santen, Eds.), p. 1005. Elsevier, Amsterdam, 1989.
32. Davis, R. J., and Derouane, E. G., *J. Catal.* **132,** 269 (1991).
33. Paál, Z., and Tétényi, P., *J. Catal.* **30,** 350 (1973).
34. Manninger, I., Xu, X. L., Tétényi, P., and Paál, Z., *Appl. Catal.* **51,** L7 (1989).
35. Barron, Y., Maire, G., Muller, J. M., and Gault, F. G., *J. Catal.* **5,** 428 (1966).
36. Paál, Z., *Catal. Today* **2,** 595 (1988).
37. Christoffel, E. G., and Paál, Z., *J. Catal.* **73,** 30 (1982).